Optimization of noise-induced synchronization of oscillator networks

Yoji Kawamura*
Department of Mathematical Science and Advanced Technology, Japan Agency for Marine-Earth Science and Technology, Yokohama 236-0001, Japan
and Research and Development Center for Marine Biosciences, Japan Agency for Marine-Earth Science and Technology, Yokosuka 237-0061, Japan

Hiroya Nakao
Department of Systems and Control Engineering, Tokyo Institute of Technology, Tokyo 152-8552, Japan
(Received 14 June 2016; published 2 September 2016)

We investigate common-noise-induced synchronization between two identical networks of coupled phase oscillators exhibiting fully locked collective oscillations. Using the collective phase description method for fully locked oscillators, we demonstrate that two noninteracting networks of coupled phase oscillators can exhibit in-phase synchronization between the networks when driven by weak common noise. We derive the Lyapunov exponent characterizing the relaxation time for synchronization and develop a method of obtaining the optimal input pattern of common noise to achieve fast synchronization. We illustrate the theory using three representative networks with heterogeneous, global, and local coupling. The theoretical results are validated by direct numerical simulations.

DOI: 10.1103/PhysRevE.94.032201

I. INTRODUCTION

An assembly of self-sustained oscillators can exhibit a rich variety of synchronization phenomena [1–19]. Among them, it is remarkable that uncoupled limit-cycle oscillators subject to weak common noise can undergo in-phase synchronization. This phenomenon is called the common-noise-induced synchronization [20–27]. Here, each oscillatory element is described by a stable limit-cycle solution to an ordinary differential equation, and the phase description method for ordinary limit-cycle oscillators [1–3,6–12] has been used successfully to explain the synchronization mechanism. On the basis of the phase description, methods of optimizing the phase-response properties of limit-cycle oscillators to realize efficient common-noise-induced synchronization have also been developed [28–31,73].

Recently, the concept of common-noise-induced synchronization has been extended to the following situations. In Ref. [40], we investigated common-noise-induced synchronization between two noninteracting populations of globally coupled oscillators exhibiting coherent collective oscillations. Here, the collective oscillation of each population is described by a stable traveling solution to a nonlinear Fokker-Planck equation representing phase-coherent states in globally coupled noisy oscillators. Similar analysis has also been performed for a model of neural activity waves by Kilpatrick in Ref. [41]. In Ref. [42], we investigated common-noise-induced synchronization between two noninteracting Hele-Shaw cells exhibiting oscillatory convection. Here, oscillatory convection is described by a stable limit-cycle solution to a partial differential equation representing the dynamics of the temperature field in the Hele-Shaw cell.

In this paper, as another, physically distinct situation, we theoretically investigate common-noise-induced collective-phase synchronization between two noninteracting systems of coupled individual-phase oscillators exhibiting fully locked states. Using the collective phase description method for fully locked states, we demonstrate that two noninteracting systems of oscillator networks can be in-phase synchronized when driven by weak common noise. Furthermore, we develop a method of obtaining the optimal input pattern of common noise to achieve fast synchronization and also derive an analytical approximation formula for the optimal input pattern. The theory is illustrated using three representative oscillator networks with heterogeneous, global, and local coupling. We also validate the theoretical results by direct numerical simulations of the three oscillator networks.

This paper is organized as follows. In Sec. II, we briefly review the collective phase description of fully locked states. In Secs. III and IV, we theoretically and numerically analyze common-noise-induced synchronization of phase oscillator networks, respectively. Concluding remarks are given in Sec. V.

II. COLLECTIVE PHASE DESCRIPTION OF OSCILLATOR NETWORKS

In this section, for the sake of readability, we summarize the collective phase description method for fully locked states in networks of coupled noiseless nonidentical oscillators. More details and other applications of this collective phase description method are given in Refs. [43–46]. See also Refs. [47–50] for related studies on the phase response and frequency precision of coupled oscillator networks.

We consider a system of coupled phase oscillators described by the following equation for $j = 1,2,\ldots,N$:

$$\dot{\phi}_j(t) = \omega_j + \sum_{k=1}^{N} \Gamma_{jk}(\phi_j - \phi_k) + \epsilon Z(\phi_j) p_j(t), \qquad (1)$$

*ykawamura@jamstec.go.jp

where $\phi_j(t) \in \mathbb{S}^1$ is the phase of the jth oscillator at time t in the system consisting of N oscillators, and ω_j is the natural frequency of the jth oscillator. The second term on the right-hand side represents the phase coupling between the oscillators, and the third term represents the effect of a weak external forcing applied to each oscillator [74]. The phase sensitivity function $Z(\phi_j)$ and phase coupling function $\Gamma_{jk}(\phi_j - \phi_k)$ are 2π-periodic functions. The external forcing is denoted by $p_j(t)$, and the characteristic intensity of the external forcing is given by $\epsilon \geqslant 0$. When the external forcing is absent, i.e., $\epsilon = 0$, Eq. (1) is assumed to have a stable fully phase-locked solution [7,8,52,53],

$$\phi_j(t) = \Theta(t) + \psi_j, \quad \dot{\Theta}(t) = \Omega, \tag{2}$$

where $\Theta(t) \in \mathbb{S}^1$ is the collective phase of the system at time t, Ω denotes the collective frequency, and the constant ψ_j represents the relative phase of each individual oscillator in the fully locked state. The collective frequency Ω is given by

$$\Omega = \omega_j + \sum_{k=1}^{N} \Gamma_{jk}(\psi_j - \psi_k), \tag{3}$$

which should be satisfied for arbitrary j.

When the external forcing is sufficiently weak, i.e., $\epsilon \ll 1$, the system of oscillators described by Eq. (1) is always near the fully phase-locked solution, Eq. (2). Therefore, we can approximately derive an equation for the collective phase $\Theta(t)$ in the following form [43]:

$$\dot{\Theta}(t) = \Omega + \epsilon \sum_{j=1}^{N} Z_j(\Theta) p_j(t), \tag{4}$$

where

$$Z_j(\Theta) = v_j Z(\Theta + \psi_j). \tag{5}$$

Here, v_j is the jth component of the left zero eigenvector associated with the constant Jacobi matrix L_{jk} of Eq. (1) for the fully phase-locked solution, Eq. (2), and the summation of v_j over the index j is normalized to unity, i.e.,

$$\sum_{j=1}^{N} v_j L_{jk} = 0, \quad \sum_{j=1}^{N} v_j = 1, \tag{6}$$

where

$$L_{jk} = \delta_{jk} \sum_{l \neq j} \Gamma'_{jl}(\psi_j - \psi_l) - (1 - \delta_{jk}) \Gamma'_{jk}(\psi_j - \psi_k). \tag{7}$$

The Jacobi matrix L_{jk} takes the form of the Laplacian matrix [17,18,54–56] associated with the effective adjacency matrix, i.e., $-\Gamma'_{jk}(\psi_j - \psi_k)$. That is, the Jacobi matrix L_{jk} satisfies $\sum_{k=1}^{N} L_{jk} = 0$ for each j. Therefore, the right zero eigenvector of L_{jk} is $\mathbf{1} = (1, 1, \ldots, 1)^{\mathrm{T}}$. In Eq. (7), we have used the Kronecker delta, δ_{jk}, and derivative notation $\Gamma'_{jk}(\phi) = d\Gamma_{jk}(\phi)/d\phi$. The Jacobi matrix L_{jk} is generally asymmetric and weighted. The collective phase Θ can be written as [43]

$$\Theta = \sum_{j=1}^{N} v_j(\phi_j - \psi_j), \tag{8}$$

under linear approximation of the isochron [1–3,7,8]. The left zero eigenvector $\boldsymbol{v} = (v_1, v_2, \ldots, v_N)$, which plays an essential role in this paper, is also called the influence in Ref. [44].

In this paper, we further assume that the external forcing is described as

$$p_j(t) = a_j q(t). \tag{9}$$

That is, the node-dependence and time-dependence of the external forcing are separated. In this case, the collective phase Eq. (4) can be written in the following form:

$$\dot{\Theta}(t) = \Omega + \epsilon \zeta(\Theta) q(t), \tag{10}$$

where the *collective phase sensitivity function* is given by

$$\zeta(\Theta) = \sum_{j=1}^{N} Z_j(\Theta) a_j = \sum_{j=1}^{N} v_j Z(\Theta + \psi_j) a_j. \tag{11}$$

When both $\psi_j = 0$ and $a_j = 1$ hold for all j, that is, when the oscillators are completely synchronized and the external forcing is uniformly applied to all the oscillators, the collective phase sensitivity function coincides with the individual phase sensitivity function, i.e., $\zeta(\Theta) = Z(\Theta)$, owing to the normalization condition of v_j.

III. THEORETICAL ANALYSIS OF NOISE-INDUCED SYNCHRONIZATION

In this section, by applying the collective phase description method in Sec. II, we analytically investigate common-noise-induced synchronization between noninteracting identical systems of phase oscillator networks. In particular, we develop a method of obtaining the optimal input pattern of common noise to achieve fast noise-induced synchronization. In addition, we also derive an analytical approximation formula for the optimal input pattern.

A. Collective phase reduction and Lyapunov exponent

We consider two noninteracting systems of phase oscillator networks subject to weak common noise described by the following equation for $\sigma = 1,2$ and $j = 1,2,\ldots,N$:

$$\dot{\phi}_j^{(\sigma)}(t) = \omega_j + \sum_{k=1}^{N} \Gamma_{jk}\left(\phi_j^{(\sigma)} - \phi_k^{(\sigma)}\right) + \epsilon Z\left(\phi_j^{(\sigma)}\right) a_j \xi(t). \tag{12}$$

The common noise $\xi(t)$ is assumed to be white Gaussian noise [57–59], the statistics of which are given by

$$\langle \xi(t) \rangle = 0, \quad \langle \xi(t)\xi(s) \rangle = 2\delta(t - s). \tag{13}$$

Here, we consider the Langevin phase Eq. (12) in the Stratonovich interpretation [57–59]. We also assume that the unperturbed system exhibits stable fully phase-locked collective oscillation and that the noise intensity ϵ^2 is sufficiently weak. Then, as in Eq. (10), we can derive a collective phase equation from Eq. (12) as follows [75]:

$$\dot{\Theta}^{(\sigma)}(t) = \Omega + \epsilon \zeta(\Theta^{(\sigma)}) \xi(t), \tag{14}$$

where the collective phase sensitivity function $\zeta(\Theta)$ is given by Eq. (11). Once the collective phase Eq. (14) is obtained,

the Lyapunov exponent characterizing common-noise-induced synchronization can be derived by following the argument in Ref. [20]. From Eqs. (13) and (14), the Lyapunov exponent, which quantifies the exponential growth rate of the small difference between the two collective-phase variables, can be written in the following form:

$$\Lambda = -\frac{\epsilon^2}{2\pi}\int_0^{2\pi} d\Theta\,[\zeta'(\Theta)]^2 \leqslant 0. \tag{15}$$

Here, we have used the derivative notation $\zeta'(\Theta) = d\zeta(\Theta)/d\Theta$. Equation (15) shows that two noninteracting systems of oscillator networks can be in-phase synchronized when driven by weak common noise as long as the collective-phase reduction approximation is valid. In the following subsection, we develop a method of obtaining the optimal input pattern of common noise to achieve fast noise-induced synchronization of phase oscillator networks.

B. Optimal input pattern of common noise

From Eq. (11), the integrand in Eq. (15) is given by

$$[\zeta'(\Theta)]^2 = \sum_{j=1}^{N}\sum_{k=1}^{N} v_j v_k Z'(\Theta+\psi_j)Z'(\Theta+\psi_k)a_j a_k, \tag{16}$$

where $Z'(\phi) = dZ(\phi)/d\phi$. From Eqs. (15) and (16), the negative of the Lyapunov exponent normalized by the noise intensity, $-\Lambda/\epsilon^2$, can be written in the following form:

$$-\frac{\Lambda}{\epsilon^2} = \frac{1}{2\pi}\int_0^{2\pi} d\Theta\,[\zeta'(\Theta)]^2 = \sum_{j=1}^{N}\sum_{k=1}^{N} K_{jk}a_j a_k, \tag{17}$$

where each element of the symmetric matrix $\hat{K}$ is given by

$$K_{jk} = \frac{v_j v_k}{2\pi}\int_0^{2\pi} d\Theta\, Z'(\Theta+\psi_j)Z'(\Theta+\psi_k) = K_{kj}. \tag{18}$$

Considering the 2π-periodicity of the phase sensitivity function $Z(\phi)$, we introduce the following Fourier series:

$$Z(\phi) = \sum_{n=-\infty}^{\infty} Z_n e^{in\phi}. \tag{19}$$

Substituting Eq. (19) into Eq. (18), we obtain

$$K_{jk} = 2v_j v_k \sum_{n=1}^{\infty} n^2 |Z_n|^2 \cos[n(\psi_j - \psi_k)] = K_{kj}. \tag{20}$$

By defining an N-dimensional column vector $\boldsymbol{a} \equiv (a_1, a_2, \ldots, a_N)^{\mathrm{T}}$, Eq. (17) can also be written as

$$-\frac{\Lambda}{\epsilon^2} = \sum_{j=1}^{N}\sum_{k=1}^{N} K_{jk}a_j a_k = \boldsymbol{a}\cdot\hat{K}\boldsymbol{a}, \tag{21}$$

which is a quadratic form. By maximizing the negative of normalized Lyapunov exponent, Eq. (21), we seek the optimal input pattern of common noise for fast synchronization. As a constraint, we introduce the following condition:

$$\boldsymbol{a}\cdot\boldsymbol{a} = \sum_{j=1}^{N} a_j^2 = 1. \tag{22}$$

That is, the total power of the input pattern is fixed at unity. Under this constraint, we consider the maximization of Eq. (21). For this purpose, we define the Lagrangian $F(\boldsymbol{a},\lambda)$ as

$$F(\boldsymbol{a},\lambda) = \sum_{j=1}^{N}\sum_{k=1}^{N} K_{jk}a_j a_k - \lambda\left(\sum_{j=1}^{N} a_j^2 - 1\right), \tag{23}$$

where the Lagrange multiplier is denoted by λ. Setting the derivative of the Lagrangian $F(\boldsymbol{a},\lambda)$ to zero, we can obtain the following equations:

$$\frac{\partial F}{\partial a_l} = 2\left(\sum_{k=1}^{N} K_{lk}a_k - \lambda a_l\right) = 0, \tag{24}$$

$$\frac{\partial F}{\partial \lambda} = -\left(\sum_{j=1}^{N} a_j^2 - 1\right) = 0, \tag{25}$$

which are equivalent to the eigenvalue problem described by

$$\hat{K}\boldsymbol{a}_\mu = \lambda_\mu \boldsymbol{a}_\mu, \quad \boldsymbol{a}_\mu\cdot\boldsymbol{a}_\mu = 1, \tag{26}$$

for $\mu = 1,2,\ldots,N$. These eigenvectors $\boldsymbol{a}_\mu$ and the corresponding eigenvalues λ_μ satisfy

$$F(\boldsymbol{a}_\mu,\lambda_\mu) = \lambda_\mu. \tag{27}$$

Because the matrix $\hat{K}$ is symmetric, the eigenvalues λ_μ are real numbers. Consequently, under the constraint given by Eq. (22), the optimal input pattern that maximizes Eq. (21) coincides with the eigenvector associated with the largest eigenvalue, i.e.,

$$\lambda_{\mathrm{opt}} = \max_{\mu}\,\lambda_\mu. \tag{28}$$

From Eq. (21), the Lyapunov exponent Λ_{opt} for the optimal pattern is given by

$$-\frac{\Lambda_{\mathrm{opt}}}{\epsilon^2} = \boldsymbol{a}_{\mathrm{opt}}\cdot\hat{K}\boldsymbol{a}_{\mathrm{opt}} = \lambda_{\mathrm{opt}}, \tag{29}$$

where $\boldsymbol{a}_{\mathrm{opt}}$ is the eigenvector associated with the eigenvalue λ_{opt}. Finally, we note that this optimization method can also be considered as finding the first principal component [65] of the quantity $Z'_j(\Theta) = v_j Z'(\Theta+\psi_j)$ for $j = 1,2,\ldots,N$. A similar optimization method has also been applied to noise-induced synchronization of oscillatory convection in Refs. [42,76].

C. Analytical approximation of the optimal input pattern

In this subsection, we derive an analytical approximation formula for the optimal input pattern by making use of the simple functional form of the quantity $Z'_j(\Theta) = v_j Z'(\Theta+\psi_j)$. The formula has a simple analytical relation to the left zero eigenvector of the Jacobi matrix and therefore gives us theoretical insights into how the optimal input pattern should be for fast synchronization. Here, we assume that the relative phase values are close to each other, i.e.,

$$\psi_j \simeq \psi_k, \tag{30}$$

which yields

$$\cos[n(\psi_j - \psi_k)] \simeq 1, \tag{31}$$

and also gives the following approximation of Eq. (5): $Z_j(\Theta) = v_j Z(\Theta + \psi_j) \simeq v_j Z(\Theta + \Theta_0)$, where Θ_0 is a constant. Thus, under the assumption given by Eq. (30), the symmetric matrix $\hat{K}$ in Eq. (20) can be approximated by the following matrix $\hat{V}$:

$$K_{jk} \simeq V_{jk} \equiv c v_j v_k, \quad c \equiv 2\sum_{n=1}^{\infty} n^2 |Z_n|^2. \tag{32}$$

As we explain below, the eigenvector associated with the largest eigenvalue of $\hat{V}$ is proportional to the transpose of the left zero eigenvector associated with the Jacobi matrix as follows:

$$\boldsymbol{a}_{\rm app} = \frac{\boldsymbol{v}^{\rm T}}{\rho}, \quad \widetilde{\lambda}_{\rm app} = c\rho^2, \quad \rho^2 \equiv \sum_{j=1}^{N} v_j^2. \tag{33}$$

Here, ρ^2 is the same as the quantity called the collective fluctuation in Ref. [45]. The matrix $\hat{V}$ is related to the following projection matrix $\hat{P}$:

$$P_{jk} \equiv \frac{V_{jk}}{\widetilde{\lambda}_{\rm app}} = \frac{v_j v_k}{\rho^2}, \quad \sum_{l=1}^{N} P_{jl} P_{lk} = P_{jk}. \tag{34}$$

According to the linear algebra [66,67], the projection matrix $\hat{P}$ possesses a single unit eigenvalue with the eigenvector parallel to $\boldsymbol{v}^{\rm T}$ and $N-1$ zero eigenvalues with eigenvectors perpendicular to $\boldsymbol{v}^{\rm T}$. Therefore, it is ensured that $\widetilde{\lambda}_{\rm app}$ is the unique largest eigenvalue of $\hat{V}$. Finally, the Lyapunov exponent $\Lambda_{\rm app}$ for the approximate input pattern is given by

$$-\frac{\Lambda_{\rm app}}{\epsilon^2} = \boldsymbol{a}_{\rm app} \cdot \hat{K} \boldsymbol{a}_{\rm app} \equiv \lambda_{\rm app} \simeq \widetilde{\lambda}_{\rm app}. \tag{35}$$

Note that $\lambda_{\rm app}$ is generally not an eigenvalue of $\hat{K}$, whereas $\widetilde{\lambda}_{\rm app}$ is an eigenvalue (the unique largest eigenvalue) of $\hat{V}$.

We here consider the special case in which the Jacobi matrix given in Eq. (7) is balanced [56], i.e., $\sum_{l\neq j} L_{jl} = \sum_{l\neq j} L_{lj}$ for each j. In this case, $\sum_{j=1}^{N} L_{jk} = 0$ holds for each k; thus, the left zero eigenvector of the Jacobi matrix L_{jk} that takes the form of the balanced Laplacian matrix is given as follows [44,45]:

$$\boldsymbol{v} = \frac{\boldsymbol{1}^{\rm T}}{N}. \tag{36}$$

Therefore, the analytical approximation Eq. (33) for this case yields

$$\boldsymbol{a}_{\rm uni} = \frac{\boldsymbol{1}}{\sqrt{N}}, \tag{37}$$

which gives a uniform input pattern. Finally, the Lyapunov exponent $\Lambda_{\rm uni}$ for the uniform input pattern is written in the following form:

$$-\frac{\Lambda_{\rm uni}}{\epsilon^2} = \boldsymbol{a}_{\rm uni} \cdot \hat{K} \boldsymbol{a}_{\rm uni} = \sum_{j=1}^{N}\sum_{k=1}^{N} \frac{K_{jk}}{N} \equiv \lambda_{\rm uni}. \tag{38}$$

Note that $\lambda_{\rm uni}$ is generally not an eigenvalue of $\hat{K}$. The balanced condition mentioned above is necessarily satisfied when the Jacobi matrix given in Eq. (7) is symmetric, i.e., $L_{jk} = L_{kj}$.

IV. NUMERICAL ANALYSIS OF NOISE-INDUCED SYNCHRONIZATION

In this section, to illustrate the theory developed in Sec. III, we numerically investigate common-noise-induced synchronization between noninteracting systems of phase oscillator networks. The numerical methods for eigenvalue problems and Langevin equations are summarized in Appendices A and B, respectively.

A. Kuramoto-Sakaguchi-type phase models

In this subsection, we summarize the definition of Kuramoto-Sakaguchi-type phase models [2,68,69], on which we focus throughout this section. First, the phase-coupling function $\Gamma_{jk}(\phi)$ is given by

$$\Gamma_{jk}(\phi) = A_{jk}\Gamma(\phi), \quad \Gamma(\phi) = -\sin(\phi + \alpha), \tag{39}$$

where the weighted symmetric adjacency matrix is denoted by $A_{jk} = A_{kj} \geqslant 0$, and the type of phase-coupling function is assumed to be in-phase coupling, i.e., $|\alpha| < \pi/2$. Second, the phase sensitivity function $Z(\phi)$ is given by

$$Z(\phi) = -\sin(\phi). \tag{40}$$

That is, a system of phase oscillator networks is written in the following form:

$$\dot{\phi}_j(t) = \omega_j - \sum_{k=1}^{N} A_{jk} \sin(\phi_j - \phi_k + \alpha) - \epsilon \sin(\phi_j) a_j \xi(t), \tag{41}$$

where we have dropped the system index σ for simplicity. In this case, the Jacobi matrix L_{jk} given in Eq. (7) is obtained as

$$\begin{aligned} L_{jk} = &-\delta_{jk} \sum_{l\neq j} A_{jl} \cos(\psi_j - \psi_l + \alpha) \\ &+ (1-\delta_{jk}) A_{jk} \cos(\psi_j - \psi_k + \alpha), \end{aligned} \tag{42}$$

which is symmetric when $\alpha = 0$ and/or when $\psi_j = \psi_k$ for any pair of j and k. In addition, the symmetric matrix K_{jk} given in Eq. (20) is obtained as

$$K_{jk} = c v_j v_k \cos(\psi_j - \psi_k), \tag{43}$$

where $c = 1/2$. Finally, the collective phase sensitivity function $\zeta(\Theta)$ is given by

$$\zeta(\Theta) = \sum_{j=1}^{N} Z_j(\Theta) a_j, \quad Z_j(\Theta) = -v_j \sin(\Theta + \psi_j). \tag{44}$$

In the following subsections, we consider several representative cases exhibiting fully locked states.

B. Case 0: Two-oscillator systems

In this subsection, we consider two-oscillator systems in which the adjacency matrix is given by $A_{12} = A_{21} = 1$ and $A_{11} = A_{22} = 0$. That is, a two-oscillator system is described by the following equations:

$$\dot{\phi}_1(t) = \omega_1 - \sin(\phi_1 - \phi_2 + \alpha) - \epsilon \sin(\phi_1) a_1 \xi(t), \tag{45}$$

$$\dot{\phi}_2(t) = \omega_2 - \sin(\phi_2 - \phi_1 + \alpha) - \epsilon \sin(\phi_2) a_2 \xi(t). \tag{46}$$

This system is the simplest case and is analytically solvable as follows. First, the phase difference in the fully locked state is determined by

$$\sin(\psi_1 - \psi_2) = \eta, \quad \eta \equiv \frac{\omega_1 - \omega_2}{2\cos\alpha}, \quad |\eta| < 1. \tag{47}$$

Second, the collective frequency Ω is obtained as

$$\Omega = \omega_1 - \eta\cos\alpha - \sqrt{1-\eta^2}\sin\alpha. \tag{48}$$

Third, the left zero eigenvector $\boldsymbol{v} = (v_1, v_2)$ is given by

$$v_1 = \frac{1}{2}\left(1 + \frac{\eta\tan\alpha}{\sqrt{1-\eta^2}}\right), \tag{49}$$

$$v_2 = \frac{1}{2}\left(1 - \frac{\eta\tan\alpha}{\sqrt{1-\eta^2}}\right). \tag{50}$$

Finally, by defining the following quantities,

$$f = v_1^2 + 2v_1v_2\eta + v_2^2, \tag{51}$$

$$g = v_1^2 - 2v_1v_2\eta + v_2^2, \tag{52}$$

the largest eigenvalue $\lambda_{\rm opt}$ can be written as

$$\lambda_{\rm opt} = \frac{v_1^2 + v_2^2 + \sqrt{fg}}{4}. \tag{53}$$

In addition, the optimal input pattern $\boldsymbol{a}_{\rm opt}$ can be obtained as

$$\boldsymbol{a}_{\rm opt} = \pm\left(\frac{x}{\sqrt{x^2+y^2}}, \frac{y}{\sqrt{x^2+y^2}}\right)^{\rm T}, \tag{54}$$

where

$$x = v_1^2 - v_2^2 + \sqrt{fg}, \tag{55}$$

$$y = 2v_1v_2\sqrt{1-\eta^2}. \tag{56}$$

Figure 1 shows the dependence of the left zero eigenvector $\boldsymbol{v}$ and optimal input pattern $\boldsymbol{a}_{\rm opt}$ on the parameter η under the phase shift $\alpha = \pi/4$. We can find that $v_1 = v_2$ and $a_1 = a_2$ when $\eta = 0$, that is, when the two oscillators are identical. Further, the signs of v_2 and a_2 simultaneously change from positive to negative as the parameter η increases, and the critical value of η under $\alpha = \pi/4$ is given by $\eta = 1/\sqrt{2} \simeq 0.7$.

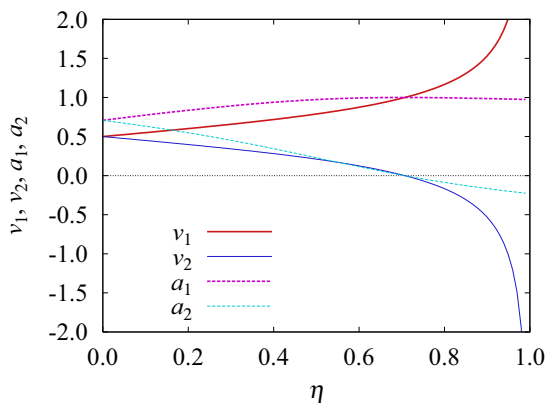

FIG. 1. Two-oscillator system. Dependence of the left zero eigenvector and optimal input pattern, i.e., v_1, v_2, a_1, and a_2, on the parameter η under the phase shift $\alpha = \pi/4$. The normalization conditions are $v_1 + v_2 = 1$ and $a_1^2 + a_2^2 = 1$.

C. Case 1: Heterogeneously coupled systems

In this subsection, we consider heterogeneously coupled systems (see also, e.g., Ref. [70]). Here, the adjacency matrix A_{jk} is generated by the Barabási-Albert model [71,72], in which the edge number of a new node to be added at each growth step and the initial node number are denoted by m and m_0, respectively. The degree d_j of the symmetric adjacency matrix A_{jk} is given by

$$d_j = \sum_{l\neq j} A_{jl} = \sum_{l\neq j} A_{lj}. \tag{57}$$

For this heterogeneously coupled system, we also consider the following input pattern:

$$\boldsymbol{a}_{\rm hub} = \mathbf{e}_h, \quad h = \arg\max_j d_j, \tag{58}$$

where the hth component of $\mathbf{e}_h$ is unity and the other components are zero. That is, common noise is applied only to the hub, which possesses the largest degree. The Lyapunov exponent $\Lambda_{\rm hub}$ for this input pattern is written in the following form:

$$-\frac{\Lambda_{\rm hub}}{\epsilon^2} = \boldsymbol{a}_{\rm hub}\cdot\hat{K}\boldsymbol{a}_{\rm hub} = K_{hh} \equiv \lambda_{\rm hub}. \tag{59}$$

Note that $\lambda_{\rm hub}$ is generally not an eigenvalue of $\hat{K}$. We also define the effective in-degree $d_j^{\rm in}$ and effective out-degree $d_j^{\rm out}$ associated with the effective adjacency matrix, $-\Gamma'_{jk}(\psi_j - \psi_k) = A_{jk}\cos(\psi_j - \psi_k)$, as follows:

$$d_j^{\rm in} = \sum_{l\neq j} A_{jl}\cos(\psi_j - \psi_l + \alpha), \tag{60}$$

$$d_j^{\rm out} = \sum_{l\neq j} A_{lj}\cos(\psi_l - \psi_j + \alpha). \tag{61}$$

Then, the Jacobi matrix can also be written in the following form: $L_{jk} = (1-\delta_{jk})A_{jk}\cos(\psi_j - \psi_k + \alpha) - \delta_{jk}d_j^{\rm in}$. As mentioned in Sec. III C, the Jacobi matrix L_{jk} is called balanced when $d_j^{\rm in} = d_j^{\rm out}$ for each j. Finally, the natural frequencies are assumed to be identical, i.e., $\omega_j = \omega$.

The network structure of the adjacency matrix A_{jk} generated by the Barabási-Albert model with $N = 100$ and $m = m_0 = 2$ and the degree d_j of the symmetric adjacency matrix A_{jk} are shown in Figs. 2(a) and 2(b), respectively. The node index is labeled in descending order of d_j; therefore, the hub is labeled $h = 1$, as shown in Fig. 2(a).

Figure 3 shows the numerical results for the heterogeneously coupled system with a phase shift of $\alpha = \pi/8$. First, the degree d_j is shown in Fig. 3(a), which is a reproduction of Fig. 2(b) for readability. Second, the relative phase ψ_j is shown in Fig. 3(b). Although the oscillators are identical, heterogeneous coupling induces phase differences between them for a nonzero phase shift, $\alpha \neq 0$. Finally, the left zero eigenvector v_j and input pattern a_j are shown in Figs. 3(c) and 3(d), respectively. Although the coupling is heterogeneous, the left zero eigenvector is almost uniform even under a nonzero phase shift, $\alpha \neq 0$; precisely speaking, the components corresponding to the high-degree nodes take

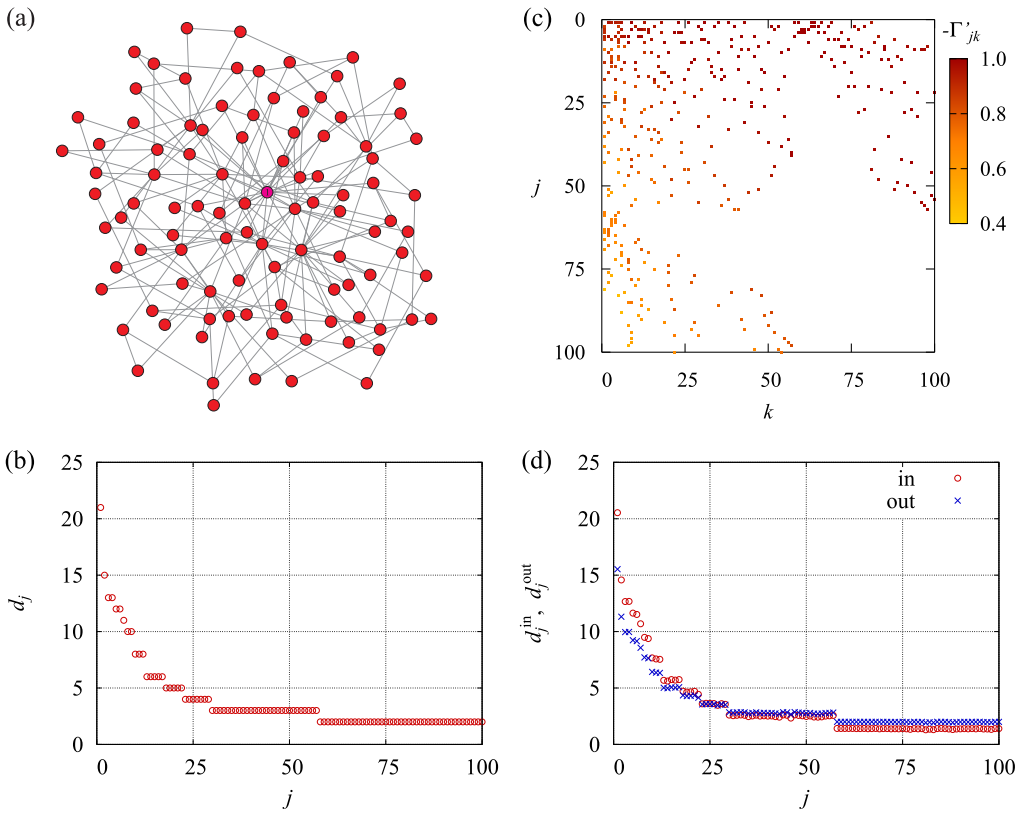

FIG. 2. Heterogeneously coupled system. The coupling network is generated by the Barabási-Albert model with $N = 100$ and $m = m_0 = 2$, the oscillators are identical, i.e., $\omega_j = \omega$, and the phase shift is $\alpha = \pi/8$. (a) Network structure associated with the symmetric adjacency matrix $A_{jk} = A_{kj}$. (b) Degree $d_j = \sum_{l\neq j} A_{jl} = \sum_{l\neq j} A_{lj}$. (c) Effective adjacency matrix, i.e., $-\Gamma'_{jk} = A_{jk}\cos(\psi_j - \psi_k + \alpha)$, in the fully locked state. (d) Effective in-degree $d_j^{\rm in} = \sum_{l\neq j} A_{jl}\cos(\psi_j - \psi_l + \alpha)$ and effective out-degree $d_j^{\rm out} = \sum_{l\neq j} A_{lj}\cos(\psi_l - \psi_j + \alpha)$.

relatively smaller values. The optimal input pattern is similar to the approximate input pattern because the relative phase values are rather close to each other.

Here, we remark on the result shown in Fig. 3(c), i.e., the left zero eigenvector v_j. The effective adjacency matrix $-\Gamma'_{jk}(\psi_j - \psi_k)$ is shown in Fig. 2(c), and also both the effective in-degree $d_j^{\rm in}$ and effective out-degree $d_j^{\rm out}$ are shown in Fig. 2(d). For small j, i.e., for the high-degree nodes, the effective in-degree $d_j^{\rm in}$ is larger than the effective out-degree $d_j^{\rm out}$. According to Refs. [44,45], the left zero eigenvector can be roughly estimated as $v_j \sim d_j^{\rm out}/d_j^{\rm in}$. Therefore, the components of $\boldsymbol{v}$ are relatively small for the high-degree nodes.

The results for the negative phase shift $\alpha = -\pi/8$ are also shown in Appendix C as Fig. 8. The left zero eigenvector $\boldsymbol{v}$ and optimal input pattern $\boldsymbol{a}_{\rm opt}$ do not depend on the sign of the phase shift α because the natural frequencies are identical, i.e., $\omega_j = \omega$.

D. Case 2: Globally coupled systems

In this subsection, we consider globally coupled systems (see also, e.g., Ref. [43]). That is, the weighted adjacency matrix is given by

$$A_{jk} = \frac{1}{N}. \tag{62}$$

The natural frequencies are assumed to be given by

$$\omega_j = \omega + \omega_\delta\left(\frac{1}{2} - \frac{j}{N}\right), \tag{63}$$

where ω_δ is the parameter of the frequency distribution. Note that ω_j is sorted in descending order.

Figure 4 shows the numerical results for the globally coupled system with the parameters $N = 100$, $\omega_\delta = 0.5$, and $\alpha = \pi/4$. First, the natural frequency ω_j and relative phase ψ_j are shown in Figs. 4(a) and 4(b), respectively. Although the coupling is global, phase differences between the oscillators exist owing to the frequency differences. Second, the left zero eigenvector v_j and input pattern a_j are shown in Figs. 4(c) and 4(d), respectively. The components of $\boldsymbol{v}$ are larger for relatively larger frequencies ω_j. The optimal input pattern is similar to the approximate input pattern because the relative phase values are rather close to each other.

The results for the negative phase shift $\alpha = -\pi/4$ are also shown in Appendix C as Fig. 9. In contrast to the case with a positive phase shift, the components of the left zero eigenvector $\boldsymbol{v}$ and optimal input pattern $\boldsymbol{a}_{\rm opt}$ are smaller for relatively larger frequencies ω_j under a negative phase shift.

E. Case 3: Locally coupled systems

In this subsection, we consider one-dimensional locally coupled systems with periodic boundary conditions (see also,

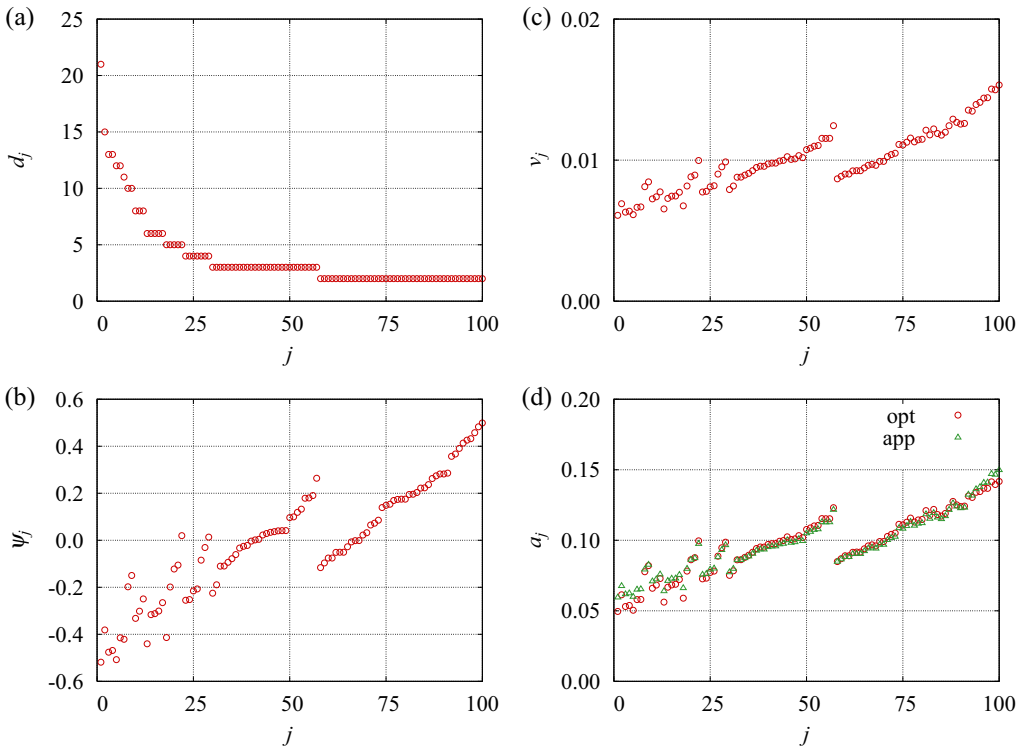

FIG. 3. Heterogeneously coupled system. The coupling network is generated by the Barabási-Albert model with $N = 100$ and $m = m_0 = 2$, the oscillators are identical, i.e., $\omega_j = \omega$, and the phase shift is $\alpha = \pi/8$. (a) Degree d_j. (b) Relative phase ψ_j. (c) Left zero eigenvector v_j. (d) Input pattern a_j. The optimal input pattern $\boldsymbol{a}_{\rm opt}$ and approximate input pattern $\boldsymbol{a}_{\rm app}$ are shown. Note that the uniform input pattern $\boldsymbol{a}_{\rm uni}$ is a vector whose components are all $1/\sqrt{N} = 0.1$. Note also that when the common noise is applied only to the hub, the input pattern is $\boldsymbol{a}_{\rm hub} = \mathbf{e}_1$.

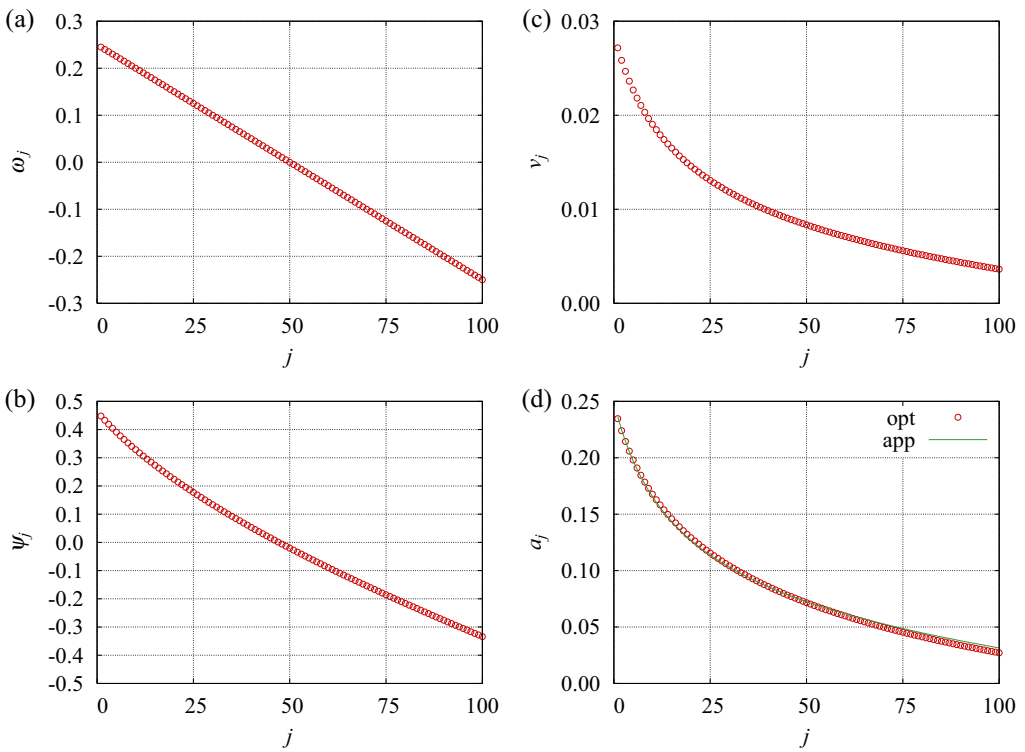

FIG. 4. Globally coupled system. The parameters are $N = 100$, $\omega_\delta = 0.5$, and $\alpha = \pi/4$. (a) Natural frequency ω_j under $\omega = 0$. (b) Relative phase ψ_j. (c) Left zero eigenvector v_j. (d) Input pattern a_j. The optimal input pattern $\boldsymbol{a}_{\rm opt}$ and approximate input pattern $\boldsymbol{a}_{\rm app}$ are shown. Note that the uniform input pattern $\boldsymbol{a}_{\rm uni}$ is a vector whose components are all $1/\sqrt{N} = 0.1$.

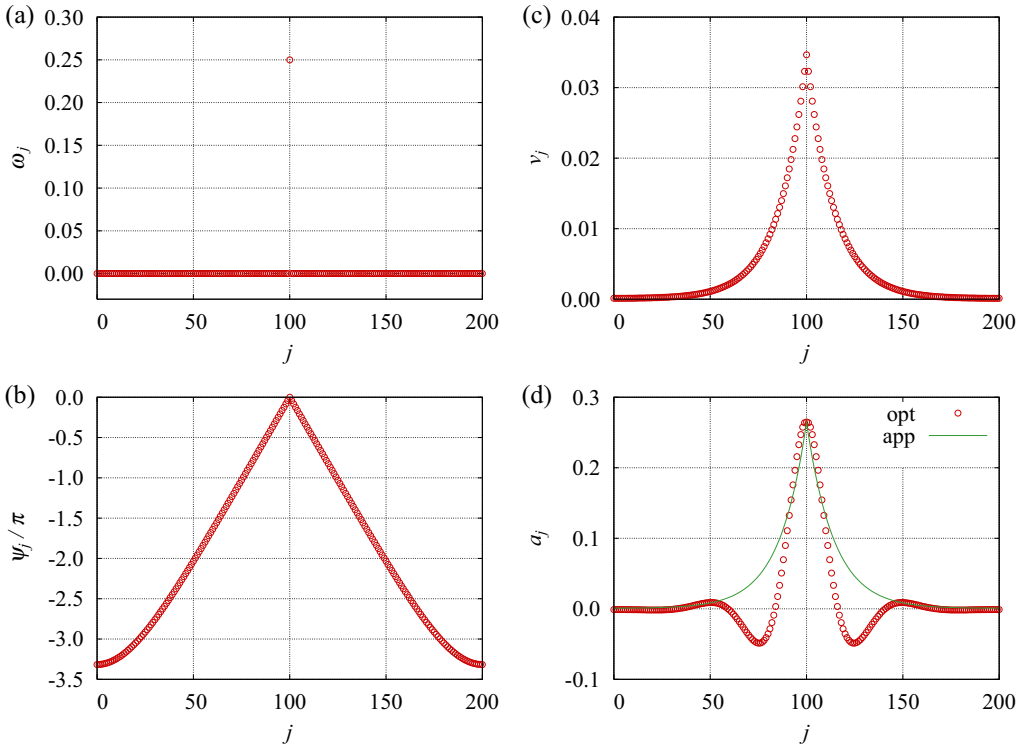

FIG. 5. Locally coupled system. The parameters are $N = 200$, $\omega_p = 0.25$, and $\alpha = \pi/12$. (a) Natural frequency ω_j under $\omega = 0$. (b) Relative phase ψ_j scaled by π. (c) Left zero eigenvector v_j. (d) Input pattern a_j. The optimal input pattern $\boldsymbol{a}_{\rm opt}$ and approximate input pattern $\boldsymbol{a}_{\rm app}$ are shown. Note that the uniform input pattern $\boldsymbol{a}_{\rm uni}$ is a vector whose components are all $1/\sqrt{N} \simeq 0.07$.

e.g., Ref. [45]). That is, the adjacency matrix is given by

$$A_{jk} = \delta_{k,\,j_+} + \delta_{k,\,j_-}, \tag{64}$$

where $j_\pm = (j \pm 1) \mod N$. The natural frequencies are assumed to be given by

$$\omega_j = \omega + \begin{cases} \omega_p & (j = N/2), \\ 0 & (j \neq N/2), \end{cases} \tag{65}$$

where ω_p is the frequency parameter of a pacemaker located at $j = N/2$.

Figure 5 shows the numerical results for the locally coupled system with the parameters $N = 200$, $\omega_p = 0.25$, and $\alpha = \pi/12$. First, the natural frequency ω_j and relative phase ψ_j are shown in Figs. 5(a) and 5(b), respectively. The relative phase depends linearly on the distance from the pacemaker located at $j = N/2$. This type of phase pattern is called the target pattern. Second, the left zero eigenvector v_j and input pattern a_j are shown in Figs. 5(c) and 5(d), respectively. The left zero eigenvector depends exponentially on the distance from the pacemaker located at $j = N/2$ and is localized near the pacemaker. Because the relative phases broaden owing to the phase waves from the pacemaker, the optimal input pattern differs significantly from the approximate input pattern. That is, the optimal input pattern shows an exponential decay with oscillations, whereas the approximate input pattern (i.e., the left zero eigenvector) decays monotonously.

Figure 6 shows snapshots of $NZ_j(\Theta) = -Nv_j \sin(\Theta + \psi_j)$ for several values of the collective phase Θ. Each snapshot shows oscillation as a function of j owing to the broad range of relative phases ψ_j; this oscillatory behavior of the locally coupled system is in sharp contrast to the behavior of the heterogeneously and globally coupled systems, in which the relative phase values are rather close to each other. The optimal input pattern is the first principal component of $Z'_j(\Theta) = -v_j \cos(\Theta + \psi_j)$, as mentioned in Sec. III B, so the optimal input pattern shows an exponential decay with oscillations, as in the snapshot of $Z_j(\Theta)$ or $Z'_j(\Theta)$.

F. Direct numerical simulations

In this subsection, we demonstrate common-noise-induced collective-phase synchronization between two noninteracting

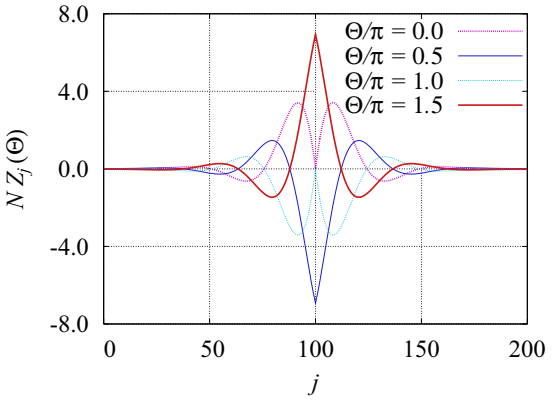

FIG. 6. Locally coupled system. Snapshots of $NZ_j(\Theta) = -Nv_j \sin(\Theta + \psi_j)$ for $\Theta/\pi = 0.0$, 0.5, 1.0, and 1.5. The parameters are $N = 200$, $\omega_p = 0.25$, and $\alpha = \pi/12$.

TABLE I. Theoretical values of the negative of normalized Lyapunov exponent $\lambda = -\Lambda/\epsilon^2 = \boldsymbol{a}\cdot\hat{K}\boldsymbol{a}$ for several input patterns (i.e., $\boldsymbol{a}_{\rm opt}, \boldsymbol{a}_{\rm app} = \boldsymbol{v}^{\rm T}/\rho, \boldsymbol{a}_{\rm uni} = \mathbf{1}/\sqrt{N}$, and $\boldsymbol{a}_{\rm hub} = \mathbf{e}_h$). (a) Heterogeneously coupled system (hetero). (b) Globally coupled system (global). (c) Locally coupled system (local).

	(a) Hetero	(b) Global	(c) Local
$\lambda_{\rm opt}$	0.004974816	0.006378432	0.006332761
$\lambda_{\rm app}$	0.004968868	0.006374346	0.004601817
$\lambda_{\rm uni}$	0.004731548	0.004766305	0.000547244
$\lambda_{\rm hub}$	0.000018504	N/A	N/A

systems of coupled individual-phase oscillators by direct numerical simulations of the Langevin-type Eq. (12). Table I summarizes the theoretical values of the negative of normalized Lyapunov exponent $\lambda = -\Lambda/\epsilon^2 = \boldsymbol{a}\cdot\hat{K}\boldsymbol{a}$ for several input patterns (i.e., $\boldsymbol{a}_{\rm opt}$, $\boldsymbol{a}_{\rm app} = \boldsymbol{v}^{\rm T}/\rho$, $\boldsymbol{a}_{\rm uni} = \mathbf{1}/\sqrt{N}$, and $\boldsymbol{a}_{\rm hub} = \mathbf{e}_h$). The parameter values for the heterogeneously, globally, and locally coupled systems are the same as those used in Figs. 3, 4, and 5, respectively.

Figure 7 shows the time evolution of the collective phase difference $|\Theta^{(1)} - \Theta^{(2)}|$. The conditions of the simulation were as follows. First, the initial value of the collective phase difference was $|\Theta_1(t=0) - \Theta_2(t=0)| = 10^{-1}$. Second, the base frequency ω was chosen such that the collective frequency becomes unity, i.e., $\Omega = 1$. Third, the intensity of the common noise was fixed at $\epsilon^2 = 0.0025$. Finally, the results of direct numerical simulations were averaged over 500 samples for each case in each coupled system. The simulation results quantitatively agree with the theory for all the cases.

Here, we note the following points. First, as shown in Table I(a) and Fig. 7(a), $\lambda_{\rm opt} \simeq \lambda_{\rm app} \simeq \lambda_{\rm uni} > \lambda_{\rm hub}$ for the heterogeneously coupled system; this fact is also found from Fig. 3(d), which shows that $\boldsymbol{a}_{\rm opt}$, $\boldsymbol{a}_{\rm app}$, and $\boldsymbol{a}_{\rm uni}$ are similar to each other but $\boldsymbol{a}_{\rm hub}$ differs from them. Second, as shown in Table I(b) and Fig. 7(b), $\lambda_{\rm opt} \simeq \lambda_{\rm app} > \lambda_{\rm uni}$ for the globally coupled system; this is also consistent with Fig. 4(d), which shows that $\boldsymbol{a}_{\rm opt}$ and $\boldsymbol{a}_{\rm app}$ are similar to each other but $\boldsymbol{a}_{\rm uni}$ differs from them. Finally, as shown in Table I(c) and Fig. 7(c), $\lambda_{\rm opt} > \lambda_{\rm app} > \lambda_{\rm uni}$ for the locally coupled system; this is also expected from Fig. 5(d), which shows that $\boldsymbol{a}_{\rm opt}$, $\boldsymbol{a}_{\rm app}$, and $\boldsymbol{a}_{\rm uni}$ differ from each other.

As shown in Appendix D, we can also consider common-noise-induced collective-phase synchronization between noninteracting, slightly nonidentical systems of individual-phase oscillator networks.

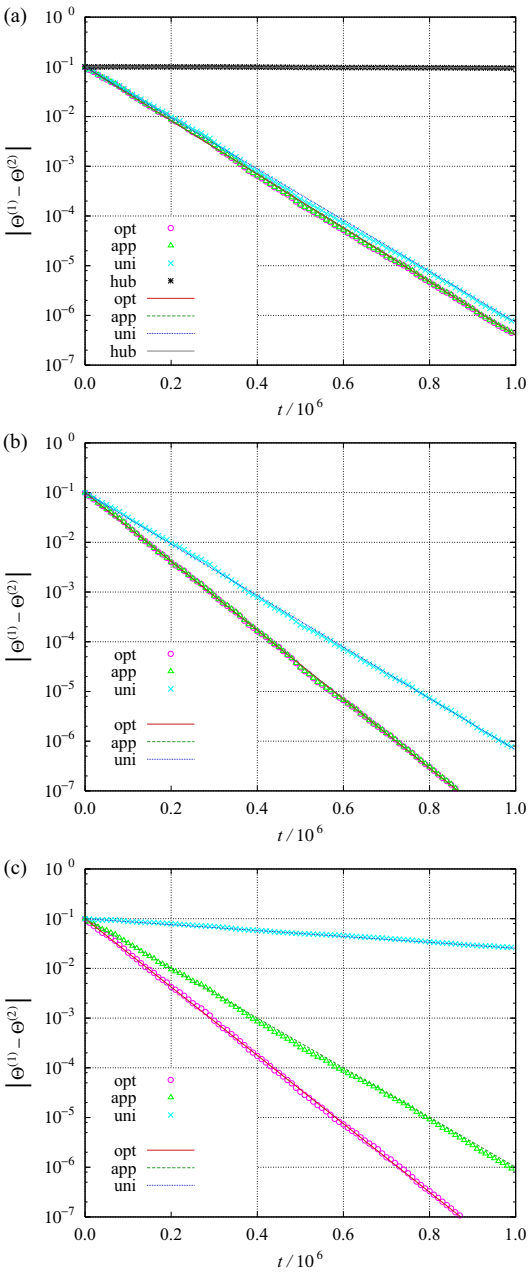

FIG. 7. Comparison of direct numerical simulations (symbols) and theoretical values (lines) of the Lyapunov exponents for several input patterns (i.e., $\boldsymbol{a}_{\rm opt}$, $\boldsymbol{a}_{\rm app}$, $\boldsymbol{a}_{\rm uni}$, and $\boldsymbol{a}_{\rm hub}$). The initial collective phase difference is $|\Theta^{(1)}(t=0) - \Theta^{(2)}(t=0)| = 10^{-1}$. The base frequency ω is chosen such that the collective frequency becomes unity, $\Omega = 1$. The noise intensity is $\epsilon^2 = 0.0025$. The results of direct numerical simulations are averaged over 500 samples. (a) Heterogeneously coupled system. (b) Globally coupled system. (c) Locally coupled system.

V. CONCLUDING REMARKS

Our investigations in this paper are summarized as follows. In Sec. II, we briefly reviewed the collective phase description method for fully locked states. In Sec. III, we analytically investigated common-noise-induced collective-phase synchronization between two noninteracting identical networks of coupled individual-phase oscillators and, in particular, developed an optimization method for noise-induced synchronization. In Sec. IV, supplemented by Appendices A, B, C, and D, we numerically investigated the common-noise-induced collective-phase synchronization and successfully validated the theoretical results by direct numerical simulations.

We also summarize the applicability of the approximate input pattern given in Eq. (33), i.e., $\boldsymbol{a}_{\rm app} = \boldsymbol{v}^{\rm T}/\rho$. The assumption for deriving the approximate input pattern is given by Eq. (30), i.e., $\psi_j \simeq \psi_k$, which means that the relative phase values are close to each other. Under this assumption, Eq. (5) can

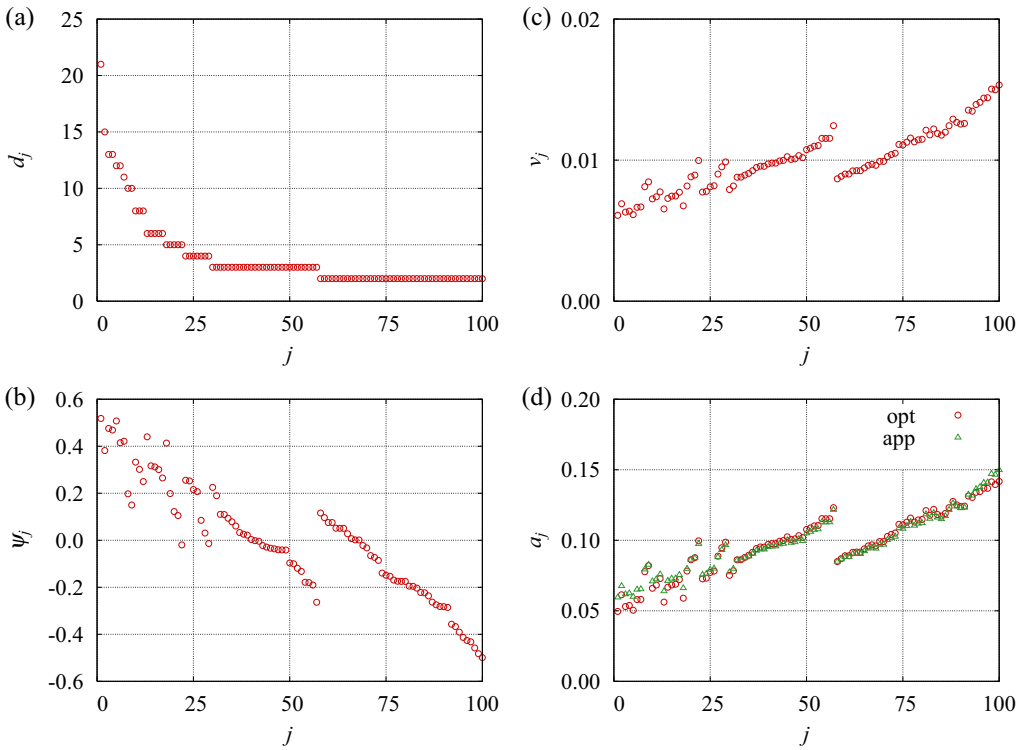

FIG. 8. Heterogeneously coupled system with a negative phase shift. The coupling network is generated by the Barabási-Albert model with $N = 100$ and $m = m_0 = 2$, the oscillators are identical, i.e., $\omega_j = \omega$, and the phase shift is $\alpha = -\pi/8$. (a) Degree d_j. (b) Relative phase ψ_j. (c) Left zero eigenvector v_j. (d) Input pattern a_j. The optimal input pattern $\boldsymbol{a}_{\rm opt}$ and approximate input pattern $\boldsymbol{a}_{\rm app}$ are shown. Note that the uniform input pattern $\boldsymbol{a}_{\rm uni}$ is a vector whose components are all $1/\sqrt{N} = 0.1$. Note also that when the common noise is applied only to the hub, the input pattern is $\boldsymbol{a}_{\rm hub} = \mathbf{e}_1$.

be approximated by $Z_j(\Theta) = v_j Z(\Theta + \psi_j) \simeq v_j Z(\Theta + \Theta_0)$, where Θ_0 is a constant; in addition, the symmetric matrix $\hat{K}$ can be approximated by Eq. (32), i.e., $K_{jk} \simeq c v_j v_k$, which gives the approximate input pattern $\boldsymbol{a}_{\rm app}$. Here, as shown in Figs. 3(d) and 8(d), the approximate input pattern is quantitatively similar to the optimal input pattern for the heterogeneously coupled system. Similarly, as shown in Figs. 4(d) and 9(d), the approximate input pattern is quantitatively similar to the optimal input pattern for the globally coupled system. However, as shown in Fig. 5(d), the approximate input pattern clearly differs from the optimal input pattern for the locally coupled system, in which the relative phases ψ_j broaden, as shown in Fig. 5(b).

Here, we note that the approximate input pattern $\boldsymbol{a}_{\rm app}$ holds good as long as $\cos(\psi_j - \psi_k) > 0$ is satisfied for any pair of j and k in Kuramoto-Sakaguchi-type phase models, which provide the symmetric matrix given by Eq. (43), i.e., $K_{jk} = c v_j v_k \cos(\psi_j - \psi_k)$. In fact, as shown in Figs. 3(b) and 8(b), $|\psi_1 - \psi_N| \simeq 1.0 < \pi/2$ for the heterogeneously coupled system. Similarly, as shown in Figs. 4(b) and 9(b), $|\psi_1 - \psi_N| \simeq 0.8 < \pi/2$ for the globally coupled system. That is, for both cases, the largest relative phase difference is not very small, but the approximate input pattern is still quantitatively similar to the optimal input pattern.

Finally, we note the broad applicability of the optimization method for common-noise-induced collective-phase synchronization between noninteracting systems of oscillator networks. As long as each system exhibits fully phase-locked collective oscillations and the common noise intensity is sufficiently weak, the optimization method developed in this paper can be applied to arbitrary oscillator networks.

ACKNOWLEDGMENTS

Y.K. acknowledges financial support from JSPS KAKENHI Grants No. JP16K17769 and No. JP25800222. H.N. acknowledges financial support from JSPS KAKENHI Grants No. JP16H01538 and No. JP16K13847.

APPENDIX A: NUMERICAL METHODS FOR EIGENVALUE PROBLEMS

In this appendix, we describe the numerical methods for the two eigenvalue problems encountered in this paper. First, the left zero eigenvector of the Jacobi matrix L_{jk} can be obtained using the relaxation method for the following equation [43]:

$$\frac{d}{dt} v_k(t) = \sum_{j=1}^{N} v_j(t) L_{jk}, \tag{A1}$$

which can be discretized by a sufficiently small Δt as follows:

$$v_k(t_{n+1}) = v_k(t_n) + \Delta t \sum_{j=1}^{N} v_j(t_n) L_{jk}, \tag{A2}$$

where the discretized time is denoted by $t_n = n\Delta t$. The normalization condition is given by $\sum_{j=1}^{N} v_j = 1$.

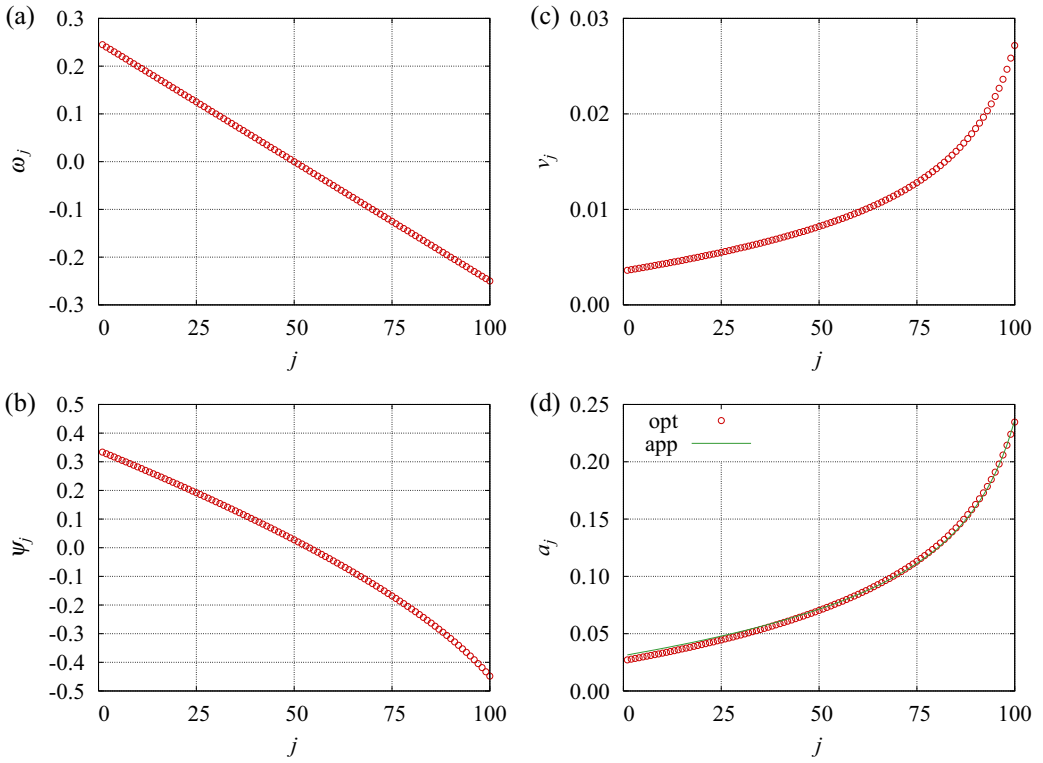

FIG. 9. Globally coupled system with a negative phase shift. The parameters are $N = 100$, $\omega_\delta = 0.5$, and $\alpha = -\pi/4$. (a) Natural frequency ω_j under $\omega = 0$. (b) Relative phase ψ_j. (c) Left zero eigenvector v_j. (d) Input pattern a_j. The optimal input pattern $\boldsymbol{a}_{\rm opt}$ and approximate input pattern $\boldsymbol{a}_{\rm app}$ are shown. Note that the uniform input pattern $\boldsymbol{a}_{\rm uni}$ is a vector whose components are all $1/\sqrt{N} = 0.1$.

Second, the eigenvector associated with the largest eigenvalue of the symmetric matrix K_{jk} can be obtained using the power method for the following equation [66,67]:

$$a_j(n+1) = \sum_{k=1}^{N} K_{jk} a_k(n), \tag{A3}$$

where the iteration count is denoted by n. The normalization condition is given by $\sum_{j=1}^{N} a_j^2 = 1$.

APPENDIX B: NUMERICAL METHODS FOR LANGEVIN EQUATIONS

In this appendix, we describe the numerical scheme for Langevin-type equations of coupled phase oscillators in the Stratonovich interpretation. The Heun scheme of Eq. (12) with Eq. (13) is given by the following equations [59]:

$$\tilde{\phi}_j^{(\sigma)}(t_{n+1}) = \phi_j^{(\sigma)}(t_n) + \Delta t\, W_j^{(\sigma)}(t_n) + \epsilon Z\big(\phi_j^{(\sigma)}(t_n)\big) a_j \chi_n, \tag{B1}$$

$$\phi_j^{(\sigma)}(t_{n+1}) = \phi_j^{(\sigma)}(t_n) + \frac{\Delta t}{2}\big[W_j^{(\sigma)}(t_n) + \tilde{W}_j^{(\sigma)}(t_{n+1})\big] + \frac{\epsilon}{2}\big[Z\big(\phi_j^{(\sigma)}(t_n)\big) + Z\big(\tilde{\phi}_j^{(\sigma)}(t_{n+1})\big)\big] a_j \chi_n, \tag{B2}$$

where

$$W_j^{(\sigma)}(t_n) = \omega_j + \sum_{k=1}^{N} \Gamma_{jk}\big(\phi_j^{(\sigma)}(t_n) - \phi_k^{(\sigma)}(t_n)\big), \tag{B3}$$

$$\tilde{W}_j^{(\sigma)}(t_{n+1}) = \omega_j + \sum_{k=1}^{N} \Gamma_{jk}\big(\tilde{\phi}_j^{(\sigma)}(t_{n+1}) - \tilde{\phi}_k^{(\sigma)}(t_{n+1})\big), \tag{B4}$$

and

$$\langle \chi_n \rangle = 0, \quad \langle \chi_n \chi_m \rangle = 2\Delta t\, \delta_{n,m}. \tag{B5}$$

The discretized time and random number are denoted by $t_n = n\Delta t$ and $\chi_n \in \mathcal{N}(0, 2\Delta t)$, respectively. From Eq. (8), the collective phase difference can be approximated by

$$\Theta^{(1)} - \Theta^{(2)} = \sum_{j=1}^{N} v_j\big(\phi_j^{(1)} - \phi_j^{(2)}\big) \simeq \phi_{j_0}^{(1)} - \phi_{j_0}^{(2)}, \tag{B6}$$

where j_0 is an arbitrary integer within $\{1, 2, \ldots, N\}$.

APPENDIX C: SYSTEMS WITH NEGATIVE PHASE SHIFTS

In this appendix, we consider heterogeneously and globally coupled systems with negative phase shifts. The parameter values are the same as those used in Sec. IV except for the phase shifts.

Figure 8 shows the numerical results for the heterogeneously coupled system with a phase shift of $\alpha = -\pi/8$. First, the degree d_j is shown in Fig. 8(a), which is a reproduction of Fig. 3(a) for readability. Second, the relative phase ψ_j is shown in Fig. 8(b). A comparison of Fig. 8(b) with Fig. 3(b) shows that the relative phase gradient for the negative phase shift is opposite to that for the positive one. Third, the left zero eigenvector v_j and input pattern a_j are shown in Figs. 8(c) and 8(d), respectively. A comparison of Figs. 8(c) and 8(d) with Figs. 3(c) and 3(d) shows that the left zero eigenvector $\boldsymbol{v}$ and optimal input pattern $\boldsymbol{a}_{\rm opt}$ do not depend on the sign of the phase shift α. This is because the natural frequencies are identical, i.e., $\omega_j = \omega$. Finally, more generally speaking, there exists the following symmetry under the reflection transform of the phase shift (i.e., $\alpha \leftrightarrow -\alpha$): $(\psi_j, v_j, a_j) \leftrightarrow (-\psi_j, v_j, a_j)$. This is because Eq. (41) with $\omega_j = \omega$ is essentially invariant under the simultaneous transformation of $\alpha \to -\alpha$ and $\phi \to -\phi$.

Figure 9 shows the numerical results for the globally coupled system with a phase shift of $\alpha = -\pi/4$. First, the natural frequency ω_j is shown in Fig. 9(a), which is a reproduction of Fig. 4(a) for readability. Second, the relative phase ψ_j is shown in Fig. 9(b). Third, the left zero eigenvector v_j and input pattern a_j are shown in Figs. 9(c) and 9(d), respectively. The left zero eigenvector $\boldsymbol{v}$ and optimal input pattern $\boldsymbol{a}_{\rm opt}$ take smaller components for relatively larger frequencies ω_j under the negative phase shift α. This is in contrast to the positive phase shift case shown in Fig. 4. Finally, more generally speaking, there exists the following symmetry under the reflection transform of the phase shift (i.e., $\alpha \leftrightarrow -\alpha$): $(\psi_j, v_j, a_j) \leftrightarrow (-\psi_{N+1-j}, v_{N+1-j}, a_{N+1-j})$. This is because Eq. (41) with Eqs. (62) and (63) is essentially invariant under the simultaneous transformation of $\alpha \to -\alpha$, $\phi \to -\phi$, and $j \to N+1-j$.

APPENDIX D: NONIDENTICAL SYSTEMS OF OSCILLATOR NETWORKS

In this appendix, we consider common-noise-induced synchronization between noninteracting, slightly nonidentical systems of phase oscillator networks described by the following equation for $\sigma = 1,2$ and $j = 1,2,\ldots,N$:

$$\dot{\phi}_j^{(\sigma)}(t) = \omega_j^{(\sigma)} + \sum_{k=1}^{N} \Gamma_{jk}^{(\sigma)}\left(\phi_j^{(\sigma)} - \phi_k^{(\sigma)}\right) + \epsilon Z\left(\phi_j^{(\sigma)}\right) a_j \xi(t), \tag{D1}$$

where the natural frequencies and phase-coupling functions for each system are assumed to be given by [77]

$$\omega_j^{(\sigma)} = \omega_j + \delta\tilde{\omega}_j^{(\sigma)}, \tag{D2}$$

$$\Gamma_{jk}^{(\sigma)}(\phi) = \Gamma_{jk}(\phi) + \delta\tilde{\Gamma}_{jk}^{(\sigma)}(\phi). \tag{D3}$$

The difference between the two systems is quantified by the parameter $\delta \geqslant 0$. When the difference between the two systems as well as the common noise is sufficiently small, we can derive a collective phase equation from Eq. (D1) as follows:

$$\dot{\Theta}^{(\sigma)}(t) = \Omega + \delta\tilde{\Omega}^{(\sigma)} + \epsilon\zeta(\Theta^{(\sigma)})\xi(t), \tag{D4}$$

where the collective frequency Ω and collective phase sensitivity $\zeta(\Theta)$ are given by Eqs. (3) and (11), respectively. In addition, the correction of the collective frequency for each system is given by the following equation:

$$\tilde{\Omega}^{(\sigma)} = \sum_{j=1}^{N} v_j\tilde{\omega}_j^{(\sigma)} + \sum_{j=1}^{N}\sum_{k=1}^{N} v_j\tilde{\Gamma}_{jk}^{(\sigma)}(\psi_j - \psi_k). \tag{D5}$$

That is, a slight difference between the two systems results in a slight difference between the two collective frequencies. Once the collective phase Eq. (D4) is obtained, common-noise-induced synchronization between noninteracting, slightly nonidentical systems can also be analyzed by following the arguments in Refs. [22,24]. The Lyapunov exponent Λ obtained in the case of identical systems (i.e., $\delta = 0$) is also the key quantity characterizing common-noise-induced synchronization in the case of slightly nonidentical systems (i.e., $0 < \delta \ll |\Lambda|$), so the optimization method developed in this paper should work well not only for identical systems but also for slightly nonidentical systems.

[1] A. T. Winfree, *The Geometry of Biological Time*, 2nd ed. (Springer, New York, 2001).

[2] Y. Kuramoto, *Chemical Oscillations, Waves, and Turbulence* (Springer, New York, 1984; Dover, New York, 2003).

[3] A. Pikovsky, M. Rosenblum, and J. Kurths, *Synchronization: A Universal Concept in Nonlinear Sciences* (Cambridge University Press, Cambridge, 2001).

[4] S. C. Manrubia, A. S. Mikhailov, and D. H. Zanette, *Emergence of Dynamical Order: Synchronization Phenomena in Complex Systems* (World Scientific, Singapore, 2004).

[5] G. V. Osipov, J. Kurths, and C. Zhou, *Synchronization in Oscillatory Networks* (Springer, New York, 2007).

[6] F. C. Hoppensteadt and E. M. Izhikevich, *Weakly Connected Neural Networks* (Springer, New York, 1997).

[7] E. M. Izhikevich, *Dynamical Systems in Neuroscience: The Geometry of Excitability and Bursting* (MIT Press, Cambridge, MA, 2007).

[8] G. B. Ermentrout and D. H. Terman, *Mathematical Foundations of Neuroscience* (Springer, New York, 2010).

[9] G. B. Ermentrout, Type I membranes, phase resetting curves, and synchrony, Neural Comput. **8**, 979 (1996).

[10] E. Brown, J. Moehlis, and P. Holmes, On the phase reduction and response dynamics of neural oscillator populations, Neural Comput. **16**, 673 (2004).

[11] H. Nakao, Phase reduction approach to synchronization of nonlinear oscillators, Contemp. Phys. **57**, 188 (2016).

[12] P. Ashwin, S. Coombes, and R. Nicks, Mathematical frameworks for oscillatory network dynamics in neuroscience, J. Math. Neurosci. **6**, 1 (2016).
[13] S. H. Strogatz, From Kuramoto to Crawford: Exploring the onset of synchronization in populations of coupled oscillators, Physica D **143**, 1 (2000).
[14] J. A. Acebrón, L. L. Bonilla, C. J. Pérez Vicente, F. Ritort, and R. Spigler, The Kuramoto model: A simple paradigm for synchronization phenomena, Rev. Mod. Phys. **77**, 137 (2005).
[15] S. Gupta, A. Campa, and S. Ruffo, Kuramoto model of synchronization: Equilibrium and nonequilibrium aspects, J. Stat. Mech. (2014) R08001.
[16] A. Pikovsky and M. Rosenblum, Dynamics of globally coupled oscillators: Progress and perspectives, Chaos **25**, 097616 (2015).
[17] S. Boccaletti, V. Latora, Y. Moreno, M. Chavez, and D.-U. Hwang, Complex networks: Structure and dynamics, Phys. Rep. **424**, 175 (2006).
[18] A. Arenas, A. Díaz-Guilera, J. Kurths, Y. Moreno, and C. Zhou, Synchronization in complex networks, Phys. Rep. **469**, 93 (2008).
[19] F. A. Rodrigues, T. K. DM. Peron, P. Ji, and J. Kurths, The Kuramoto model in complex networks, Phys. Rep. **610**, 1 (2016).
[20] J. N. Teramae and D. Tanaka, Robustness of the Noise-Induced Phase Synchronization in a General Class of Limit Cycle Oscillators, Phys. Rev. Lett. **93**, 204103 (2004).
[21] D. S. Goldobin and A. Pikovsky, Synchronization of self-sustained oscillators by common white noise, Physica A **351**, 126 (2005).
[22] D. S. Goldobin and A. Pikovsky, Synchronization and desynchronization of self-sustained oscillators by common noise, Phys. Rev. E **71**, 045201 (2005).
[23] H. Nakao, K. Arai, and Y. Kawamura, Noise-Induced Synchronization and Clustering in Ensembles of Uncoupled Limit-Cycle Oscillators, Phys. Rev. Lett. **98**, 184101 (2007).
[24] K. Yoshimura, P. Davis, and A. Uchida, Invariance of frequency difference in nonresonant entrainment of detuned oscillators induced by common white noise, Prog. Theor. Phys. **120**, 621 (2008).
[25] W. Kurebayashi, K. Fujiwara, and T. Ikeguchi, Colored noise induces synchronization of limit cycle oscillators, Europhys. Lett. **97**, 50009 (2012).
[26] P. Zhou, S. D. Burton, N. N. Urban, and G. B. Ermentrout, Impact of neuronal heterogeneity on correlated colored noise-induced synchronization, Front. Comput. Neurosci. **7**, 113 (2013).
[27] S. Sunada, K. Arai, K. Yoshimura, and M. Adachi, Optical Phase Synchronization by Injection of Common Broadband Low-Coherent Light, Phys. Rev. Lett. **112**, 204101 (2014).
[28] S. Marella and G. B. Ermentrout, Class-II neurons display a higher degree of stochastic synchronization than class-I neurons, Phys. Rev. E **77**, 041918 (2008).
[29] A. Abouzeid and G. B. Ermentrout, Type-II phase resetting curve is optimal for stochastic synchrony, Phys. Rev. E **80**, 011911 (2009).
[30] S. Hata, K. Arai, R. F. Galán, and H. Nakao, Optimal phase response curves for stochastic synchronization of limit-cycle oscillators by common Poisson noise, Phys. Rev. E **84**, 016229 (2011).
[31] W. Kurebayashi, T. Ishii, M. Hasegawa, and H. Nakao, Design and control of noise-induced synchronization patterns, Europhys. Lett. **107**, 10009 (2014).
[32] J. Moehlis, E. Shea-Brown, and H. Rabitz, Optimal inputs for phase models of spiking neurons, J. Comput. Nonlin. Dyn. **1**, 358 (2006).
[33] T. Harada, H.-A. Tanaka, M. J. Hankins, and I. Z. Kiss, Optimal Waveform for the Entrainment of a Weakly Forced Oscillator, Phys. Rev. Lett. **105**, 088301 (2010).
[34] I. Dasanayake and J.-S. Li, Optimal design of minimum-power stimuli for phase models of neuron oscillators, Phys. Rev. E **83**, 061916 (2011).
[35] A. Zlotnik and J.-S. Li, Optimal entrainment of neural oscillator ensembles, J. Neural Eng. **9**, 046015 (2012).
[36] A. Zlotnik, Y. Chen, I. Z. Kiss, H.-A. Tanaka, and J.-S. Li, Optimal Waveform for Fast Entrainment of Weakly Forced Nonlinear Oscillators, Phys. Rev. Lett. **111**, 024102 (2013).
[37] H.-A. Tanaka, Synchronization limit of weakly forced nonlinear oscillators, J. Phys. A: Math. Theor. **47**, 402002 (2014).
[38] H.-A. Tanaka, Optimal entrainment with smooth, pulse, and square signals in weakly forced nonlinear oscillators, Physica D **288**, 1 (2014).
[39] H.-A. Tanaka, I. Nishikawa, J. Kurths, Y. Chen, and I. Z. Kiss, Optimal synchronization of oscillatory chemical reactions with complex pulse, square, and smooth waveforms signals maximizes Tsallis entropy, Europhys. Lett. **111**, 50007 (2015).
[40] Y. Kawamura, H. Nakao, K. Arai, H. Kori, and Y. Kuramoto, Collective Phase Sensitivity, Phys. Rev. Lett. **101**, 024101 (2008).
[41] Z. P. Kilpatrick, Stochastic synchronization of neural activity waves, Phys. Rev. E **91**, 040701(R) (2015).
[42] Y. Kawamura and H. Nakao, Noise-induced synchronization of oscillatory convection and its optimization, Phys. Rev. E **89**, 012912 (2014).
[43] H. Kori, Y. Kawamura, H. Nakao, K. Arai, and Y. Kuramoto, Collective-phase description of coupled oscillators with general network structure, Phys. Rev. E **80**, 036207 (2009).
[44] N. Masuda, Y. Kawamura, and H. Kori, Analysis of relative influence of nodes in directed networks, Phys. Rev. E **80**, 046114 (2009).
[45] N. Masuda, Y. Kawamura, and H. Kori, Collective fluctuations in networks of noisy components, New J. Phys. **12**, 093007 (2010).
[46] Y. Kawamura, Phase synchronization between collective rhythms of fully locked oscillator groups, Sci. Rep. **4**, 4832 (2014).
[47] T.-W. Ko and G. B. Ermentrout, Phase response curves of coupled oscillators, Phys. Rev. E **79**, 016211 (2009).
[48] R. Tönjes and B. Blasius, Perturbation analysis of complete synchronization in networks of phase oscillators, Phys. Rev. E **80**, 026202 (2009).
[49] M. C. Cross, Improving the frequency precision of oscillators by synchronization, Phys. Rev. E **85**, 046214 (2012).
[50] J.-M. A. Allen and M. C. Cross, Frequency precision of two-dimensional lattices of coupled oscillators with spiral patterns, Phys. Rev. E **87**, 052902 (2013).
[51] G. S. Schmidt, D. Wilson, F. Allgöwer, and J. Moehlis, Selective averaging with application to phase reduction and neural control, Nonlinear Theory and Its Applications IEICE **5**, 424 (2014).

[52] G. B. Ermentrout, Stable periodic solutions to discrete and continuum arrays of weakly coupled nonlinear oscillators, SIAM J. Appl. Math. **52**, 1665 (1992).
[53] R. E. Mirollo and S. H. Strogatz, The spectrum of the locked state for the Kuramoto model of coupled oscillators, Physica D **205**, 249 (2005).
[54] N. Biggs, Algebraic potential theory on graphs, Bull. London Math. Soc. **29**, 641 (1997).
[55] R. P. Agaev and P. Yu. Chebotarev, The matrix of maximum out forests of a digraph and its applications, Autom. Remote Control **61**, 1424 (2000).
[56] R. Olfati-Saber, J. A. Fax, and R. M. Murray, Consensus and cooperation in networked multi-agent systems, Proc. IEEE **95**, 215 (2007).
[57] H. Risken, *The Fokker-Planck Equation: Methods of Solution and Applications* (Springer, New York, 1989).
[58] C. W. Gardiner, *Handbook of Stochastic Methods: For Physics, Chemistry and the Natural Sciences* (Springer, New York, 1997).
[59] J. García-Ojalvo and J. M. Sancho, *Noise in Spatially Extended Systems* (Springer, New York, 1999).
[60] K. Yoshimura and K. Arai, Phase Reduction of Stochastic Limit Cycle Oscillators, Phys. Rev. Lett. **101**, 154101 (2008).
[61] J. N. Teramae, H. Nakao, and G. B. Ermentrout, Stochastic Phase Reduction for a General Class of Noisy Limit Cycle Oscillators, Phys. Rev. Lett. **102**, 194102 (2009).
[62] H. Nakao, J. N. Teramae, D. S. Goldobin, and Y. Kuramoto, Effective long-time phase dynamics of limit-cycle oscillators driven by weak colored noise, Chaos **20**, 033126 (2010).
[63] D. S. Goldobin, J. N. Teramae, H. Nakao, and G. B. Ermentrout, Dynamics of Limit-Cycle Oscillators Subject to General Noise, Phys. Rev. Lett. **105**, 154101 (2010).
[64] J. Moehlis, Improving the precision of noisy oscillators, Physica D **272**, 8 (2014).
[65] I. T. Jolliffe, *Principal Component Analysis*, 2nd ed. (Springer, New York, 2002).
[66] R. A. Horn and C. R. Johnson, *Matrix Analysis*, 2nd ed. (Cambridge University Press, Cambridge, 2012).
[67] G. H. Golub and C. F. Van Loan, *Matrix Computations*, 4th ed. (Johns Hopkins University Press, Baltimore, 2012).
[68] H. Sakaguchi and Y. Kuramoto, A soluble active rotator model showing phase transitions via mutual entrainment, Prog. Theor. Phys. **76**, 576 (1986).
[69] H. Sakaguchi, S. Shinomoto, and Y. Kuramoto, Mutual entrainment in oscillator lattices with nonvariational type interaction, Prog. Theor. Phys. **79**, 1069 (1988).
[70] T.-W. Ko and G. B. Ermentrout, Partially locked states in coupled oscillators due to inhomogeneous coupling, Phys. Rev. E **78**, 016203 (2008).
[71] A.-L. Barabási and R. Albert, Emergence of scaling in random networks, Science **286**, 509 (1999).
[72] R. Albert and A.-L. Barabási, Statistical mechanics of complex networks, Rev. Mod. Phys. **74**, 47 (2002).
[73] Optimization methods for forced synchronization have also been intensively developed in Refs. [32–39].
[74] This type of selective averaged phase equation was established in Refs. [43,51].
[75] Precisely speaking, owing to the noise, the collective frequency given in Eq. (14) can differ slightly from the collective frequency given by Eq. (3); however, this point is not essential in this paper because Eq. (15) is independent of the value of the collective frequency. The theory of stochastic phase reduction for ordinary limit-cycle oscillators has been intensively investigated in Refs. [60–64].
[76] As also mentioned in the main text, the optimization method developed in this paper can be considered as finding the first principal component of the quantity $Z'_j(\Theta) = v_j Z'(\Theta + \psi_j)$. In contrast, the optimization method developed in Ref. [42] can be considered as finding the first principal component of the quantity $\partial_\Theta Z(\boldsymbol{r},\Theta)$. We can find that the discrete node index j in this paper corresponds to the continuous space coordinate $\boldsymbol{r}$ in Ref. [42] and that the target quantity in this paper is more analytically tractable than that in Ref. [42].
[77] The difference of the phase sensitivity function between the oscillators in Eq. (D1) can be neglected owing to the smallness of the common noise intensity, i.e., $\epsilon \ll 1$.